Substrate-type Hydrogenated Amorphous SiGe Thin Film Solar Cells with Ge-graded SiGe Layers on Opaque Substrates

Yoo Jeong Lee[1,2], Kwang Hoon Jung[1,2], Jung Wook Lim[1,2] and Sun Jin Yun[1,2*]

[1]Information & Communications Core Technology Research Laboratory, Electronics and Telecommunications Research Institute, Daejeon (Korea)

[2]Department of Advanced Device Engineering, University of Science and Technology, Daejeon (Korea)

Abstract

a-SiGe:H thin film solar cells with a light-abosrbing layer having differently graded Ge-compostion (C_{Ge})-profiles were fabricated to investigate the effect of C_{Ge}-profiling on the cell performance and light-induced degradation (LID). The C_{Ge}-profiles were linear normal profiling, nonlinear normal profilings, nonlinear reverse profiling, and nonlinear U-shape profiling. The cells with these C_{Ge}-profiles were compared to the cells with a constant $C_{Ge.}$ Among the samples, the cells with normal profilings showed better performances than the others. The efficiencies of the cells with linear and nonlinear normal profilings were 6.31 and 6.10%, respectively. Compared to the cells with constant-C_{Ge}, the efficiency of the cells with normal profiling was increased mainly due to the increase in the fill factor, which could be induced by the enhancement of internal field. The light-soaking experiment also showed that C_{Ge}-profilings can reduce LID. In this work, the use of a light-absorbing layer with graded C_{Ge}-profiling could improve the cell performance in terms of both efficiency and LID.

Keywords: *substrate-type solar cell, a-SiGe:H, Ge-composition profiling, light-induced degradation, internal field*

---

1. Introduction

Thin film photovoltaic devices based on hydrogenated amorphous silicon (a-Si:H) have been extensievley investigated in efforts to achieve high conversion efficiency and low-cost production. One of the most effective approaches used to achieve high efficiency is the fabrication of multi-junction (MJ) solar cells. The nip-type MJ cells on opaque and flexible substrates such as metal sheets or plastic films have also attracted much attention due to their promising applications including building- and device-integrated solar cells. Si-based MJ solar cells usually consist of a wide bandgap a-Si:H top cell (the optical bandgap energy, E_g = 1.7 –

doi:10.18086/swc.2015.05.10 Available at http://proceedings.ises.org

1.8 eV) and narrow bandgap sub-cells. Hydrogenated microcrystalline Si (μc-Si:H) and hydrogenated amorphous silicon germanium (a-SiGe:H) are good candidates for the narrow bandgap materials because the E_g of μc-Si:H is approximately 1.1 eV (Kondo and Matsuda, 2001) and that of a-SiGe:H can be varied in the range of 1.1 – 1.8 eV by controlling the Ge-fraction (Xu et al., 1996). However, μc-Si:H film have a low deposition rate and low light absorption coefficient, which are drawbacks in view of productivity because the μc-Si:H films need to be thicker than 1.5 μm to sufficiently absorb incident sunlight (Vetterl et al., 2000; Guo et al., 1998). Therefore, a-SiGe:H films, which have high deposition rates and a high light absorption coefficient can be good alternatives for improving the productivity of MJ solar cells.

The E_g of an a-SiGe:H film can be lowered and the light absorbance in the long-wavelength region ~~is~~ can be increased by increasing the amount of the Ge-fraction. However, the defect density of a-SiGe:H films increases with Ge-content (Stutzmann et al., 1989; Beyer, 2010), and many defects at n-Si:H/i-SiGe:H and p-Si:H/i-SiGe:H interfaces are generated by band-gap discontinuities (Lundszien et al., 2002). Therefore, the incorporation of Ge adversely affects the collection of photo-generated carriers due to the decrease of drift length and the increase of recombination centers, and causes the deterioration of cell performance. Earlier studies investigating methods to reduce the bandgap discontinuity and defect density have focused on the insertion of buffer layers or Ge-composition grading at the p/i- and n/i-interface regions (Zimmer et al., 1998; Arya et al., 1989). We previously reported the effect of a-SiGe:H with linearly graded Ge-composition on solar cell performance in the relatively low Ge-composition ranging from 0 to 16% (Yun et al., 2012). The light-induced degradation (LID) effect has also been studied for a-SiGe:H thin film solar cells because LID is more severe in a-SiGe:H than a-Si:H thin film solar cells (Shima et al., 2005). The study on LID effect is very important because it is closely related to the long-term stability of the a-SiGe:H thin film solar cell module.

In the present work, the Ge-composition of a light-absorbing layer was graded throughout rather than the p/i- or n/i-interface regions, and the Ge-content was varied in the range of 0 - 33%. A Ge-content of 33% is significantly higher than the commonly used Ge-content in a-SiGe:H solar cells because the performance of cells having a Ge-content exceeding 20% has been reported to be deteriorated by defects (Jones et al., 1993). The purpose of the Ge-grading in this work is to utilize the advantage of a high Ge-content region for absorbing a wide solar spectrum and to reduce the disadvantage of defective Ge-rich region in the light-absorbing layer. The enhanced internal field which can improve the carrier collection would be caused by the Ge-composition grading throughout light-absorbing layer. We also explored the optimum Ge-grading profile to achieve high conversion efficiency of nip-type a-SiGe:H thin film solar cells, and the most effective Ge-profiling was suggested for obtaining high efficiency and long-term stability.

2. Experimental details

The nip-type a-SiGe:H single junction cells were fabricated in a single chamber plasma enhanced chemical vapor deposition (PECVD) system. The schematic structure of the a-SiGe:H solar cell is illustrated in Fig .1. Ga-doped ZnO (ZnO:Ga) layers deposited by an rf-magnetron sputtering technique were used as transparent electrodes. Ag films coated with 200 nm ZnO:Ga were used as back-reflectors. Intrinsic SiGe:H layers with a thickness of 200 nm were deposited on the n-Si:H layer at 200 ^{o}C using SiH_4 (100%), GeH_4 (1.5%, diluted in H_2) and H_2 (100%) as source gases. a-SiGe:H films with graded Ge-composition profiles were prepared by gradually varying GeH_4 flow rate from 0 to 100 sccm (normal profiling) or 100 to 0 sccm (reverse profiling). The 20 nm-thick n-Si:H and 25 nm-thick p-Si:H layers were deposited using PH_3 (1.5%, diluted in H_2) and B_2H_6 (0.5%, diluted in H_2) as doping gases. An Al grid was formed on the ZnO:Ga top electrode using an e-beam evaporation process. The cell area defined by the top electrode was 0.2 cm^2. The solar cells were characterized by solar simulator under AM 1.5G spectrum and 100 mW/cm^2 illumination intensity at room temperature. External quantum efficiency (EQE) measurement was also carried out to investigate the light-absorbing behavior of a-SiGe:H layers having different Ge-profiles. To estimate the LID, the a-SiGe:H thin film solar cells were light-soaked under 1sun at 25^{o}C for 140 h.

The Ge-composition (C_{Ge}) profiles of the a-SiGe:H films were analyzed using Auger electron spectroscopy (AES). UV-Vis spectroscopy was utilized to measure the absorbance of the a-SiGe:H films, and the E_g was determined by Tauc's plot utilizing the absorbance data.

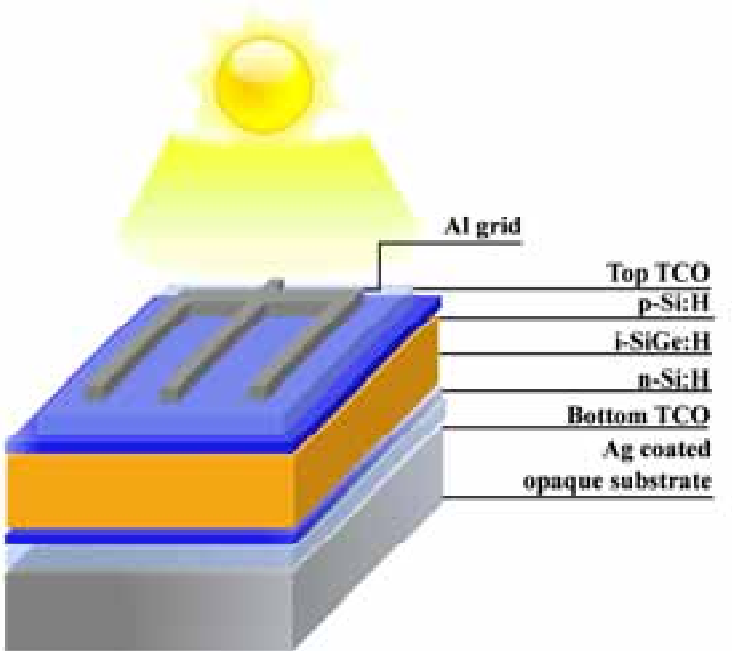

Fig. 1: Structure of the substrate-type a-SiGe:H thin film solar cells with Ge-composition profiled light-abosrbing layer.

3. Results and Discussions

First, thin film solar cells having a-SiGe:H light-absorbing layers with four different C_{Ge} profiles were fabricated to investigate the effect of Ge-profiling on cell performance. In this work, two different methods of C_{Ge}-grading were used; linear and nonlinear profilings. Cells with constant C_{Ge} in the a-SiGe:H light-absorbing layers were also fabricated to compare with the cells that had C_{Ge}-gradings.

The AES depth profiles of a-SiGe:H films with constant C_{Ge} and linear normal profiling are presented in Fig. 2(a), and those with nonlinear normal and reverse profilings are shown in Fig. 2(b). The thickness of the a-SiGe:H layer was 200 nm for all samples. The AES data in Fig. 2(a) shows that the C_{Ge} of the film deposited with GeH_4 100 sccm was approximately 33.0%, and that the Ge was uniformly distributed in the a-SiGe:H. Fig. 2(a) also shows that the C_{Ge} of the linear normal profiling sample changed linearly from approximately 33 to 0% and the average C_{Ge} in the film was 16.5%. The depth profiles of the nonlinear profilings are presented in Fig. 2(b). The C_{Ge} of the films with normal and reverse profiling decreased nonlinearly from approximately 33 to 0%, and increased from 0 to 33% in the depth direction, respectively. For the nonlinear C_{Ge}-profiled a-SiGe:H films, the average C_{Ge} was approximately 11.0% which is 5.5% smaller than that of the linear C_{Ge}-profiled film. To determine the bandgap energy (E_g) depending on the C_{Ge} of a-SiGe:H, the absorption coefficient of the films was obtained using UV-Vis spectroscopy. The E_g values of the films with C_{Ge} = 33, 16, and 0%, estimated by Tauc's plot, were 1.55, 1.66, and 1.75 eV, respectively, which were linearly decreased with respect to C_{Ge}. Then, the C_{Ge}-graded profiles correspond inversely to the E_g-graded profiles.

As briefly explained in the introduction section, the purpose of C_{Ge}-grading is to absorb a wide solar spectrum and to reduce the disadvantage of a Ge-rich region. However, to obtaining high efficiency, it is also very important that the C_{Ge}, i.e., E_g should be profiled to effectively collect carriers.

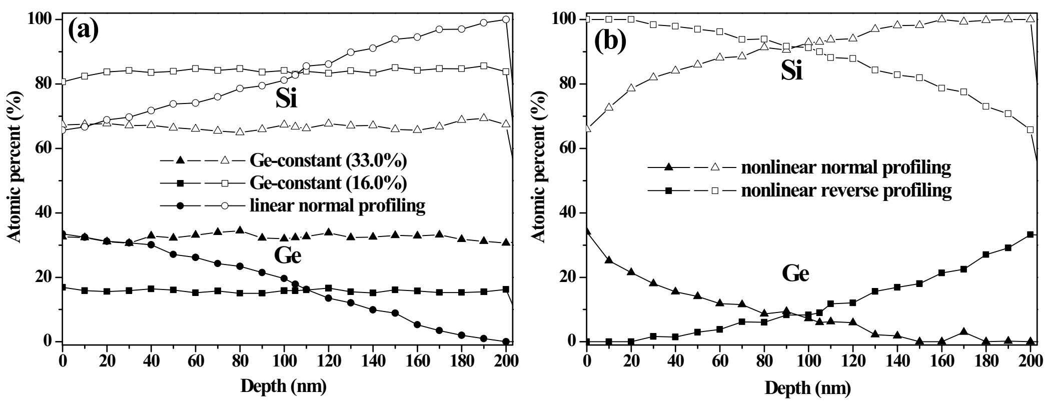

Fig. 2: AES depth profiles of a-SiGe:H films of (a) constant (33 and 16 %) and linearly graded C_{Ge} (33 - 0%) and (b) nonlinearly graded C_{Ge}-profiles (0-33 % or 33-0 %).

Figure 3 shows the schematic band-diagrams of thin film solar cells having a light-absorbing layer with E_g-profiles. As denoted by the arrows in the band-diagrams, the photo-generated holes and electrons are collected through p- and n-layers, respectively. The internal field in the light-absorbing layer with the E_g-profile could be enhanced either in view of hole or electron drift (Zambrano et al., 2004). The band-diagram of Fig. 3(a) shows that normal profiling can strengthen the internal field toward the p-layer and this allows holes to transport effectively from the n-side to the p-side in comparison to that of the E_g-constant light-absorbing layer denoted by the dotted line. On the other hand, the reverse profiling of Fig. 3(b) can enhance the internal field in the opposite direction to hole collection. With U-shape profiling, which is the complex structure of (a) and (b) as shown in Fig. 3(c), the additional internal field generates in the opposite direction to the carrier collections at both the p/i- and n/i-interface regions.

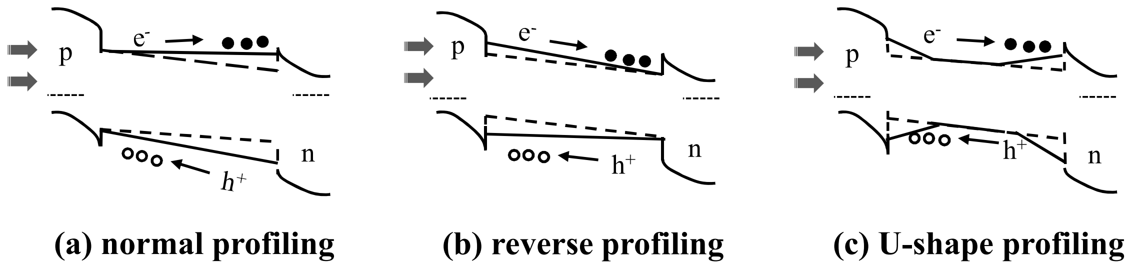

Fig. 3: Energy band-diagrams of the nip-type a-SiGe:H solar cells with (a) normal profiling, (b) reverse profiling, and (c) U-shape profiling; the dotted lines indicate the band-diagram of the cell with Ge-constant (33%).

For a-SiGe:H thin film solar cells, it has been reported that efficiency is limited by the collection of holes because the lifetime of holes is much shorter than electrons. Therefore, among the profilings shown in Fig. 3, the normal profiling is expected to be the most advantageous for the collection of holes in the nip-type a-SiGe:H solar cells fabricated in the present work.

To investigate which profiling is effective for obtaining high efficiency in practical a-SiGe:H thin film solar cells, single junction a-SiGe:H solar cells having different C_{Ge}-profiles were fabricated on opaque substrates. The cell performances are summarized in Table 1. The cell with linear normal profiling (Cell C) showed the highest conversion efficiency (η) of 6.30%. The η was approximately 20 and 29% higher than the cells with C_{Ge} = 33.0% (Cell A) and 16.0% (Cell B), respectively. The improvement of η was mainly attributed to the increase of fill factor (FF) which was induced by the improved shunt resistance. Normally, a strengthened internal field causes an increase in shunt resistance. It also has been generally known that the short-circuit current density (J_{SC}) of a-SiGe:H is considerably increased with increasing C_{Ge} (Agarwal et al., 2002). However, the Jsc of Cell C (15. 65 mA/cm^2) was a little higher than Cell A (15.43 mA/cm^2) although the average C_{Ge} of Cell C (16.5%) was much lower than that of Cell A (33.0%). In the case of Cell D with nonlinear normal profiling and an average C_{Ge} = 11.0%, the η was 6.10% and the J_{SC} was only 2.3% lower than that of Cell A.

The cells with reverse profiling (Cell E) and U-shape profiling (Cell F) showed an increased V_{OC} of 0.697V. The U-shape profiling consisted of 50 nm reverse profiling, 100 nm C_{Ge}-constant (C_{Ge} = 33.0%), and 50 nm normal profiling regions. The increased V_{OC} in both Cell E and Cell F could be explained that the wide bandgap region (C_{Ge} = 0%) of the a-SiGe:H layer was interfaced to the p-layer, as illustrated in Figs. 3(b) and (c). On the other hand, the J_{SC} of Cell E was significantly lower than that of Cell A. This might be because the C_{Ge} of Cell E was much smaller than that of Cell A and it was also difficult to collect holes due to the enhanced internal field in the opposite direction, as illustrated in Fig. 3(b). The generation of additional internal field in Cell E could be indirectly supported by the increase of shunt resistance compared to Cell A and Cell B with constant C_{Ge}, as shown in Table 1. In contrast to Cell C, Cell D, and Cell E with C_{Ge}-gradings, the shunt resistance of Cell F was rather decreased due to the additional internal field generated in the p/i- and n/i-interface regions in the opposite direction.

Table 1: Performance of the a-SiGe:H solar cell with different C_{Ge}-profiles

i-SiGeH layer (graded C_{Ge} from p- to n-side)		Cell ID	V_{OC} (V)	J_{SC} (mA/cm^2)	FF (%)	η (%)	R_{Sh} (Ω)	R_S (Ω)
Constant	C_{Ge} = 33.0%	A	0.669	15.43	50.8	5.24	1000	41
	C_{Ge} = 16.0%	B	0.703	13.83	50.2	4.89	1000	48
Linear normal profiling (from 33.0 to 0%) (average C_{Ge} = 16.5%)		C	0.679	15.65	59.3	6.31	2000	34
Nonlinear normal profiling (from 33.0 to 0%) (average C_{Ge} = 11.0%)		D	0.670	15.08	60.4	6.10	2100	31
Nonlinear reverse profiling (from 0 to 33.0 %) (average C_{Ge} = 11.0%)		E	0.697	10.43	58.9	4.28	1900	38
Nonlinear U-shape profiling (from 0% (p-side) to 33.0% (50 nm), constant 33.0% (100 nm) and 33.0 - 0% (n-side) (50 nm)) (average C_{Ge} = 22.0%)		F	0.697	13.15	42.3	3.87	890	57

The influence of C_{Ge}-grading on the the light-absorbing behavior was also examined by EQE measurement. Fig. 4 shows the EQE curves of the cells whose performances are listed in Table 1. The EQE curves of the cells with linear normal profiling (Cell C), nonlinear normal profiling (Cell D), and constant C_{Ge} (Cell A (33.0%) and Cell B (16.0%)) are presented in Fig. 4(a). The EQE values of Cell C and Cell D were larger than that of Cell A and Cell B in the wavelength region (500 – 730 nm) due to the enhancement of the internal field. In the long-wavelength region (730 – 850 nm), Cell C (16.5%) and Cell D (11.0%) showed smaller EQE values than Cell A (33.0%), but the EQE values of the Cell C and Cell D were significantly larger than that of Cell B (16.0%). The result clearly showed that the EQE values of Cell C (average C_{Ge} = 16.5%) and Cell D (average C_{Ge} = 11.0%) with graded C_{Ge}-profiles greatly increased compared to that with constant C_{Ge} (Cell B, C_{Ge} = 16.0%) especially in the long-wavelength region where the light-absorption is belived to depend on the C_{Ge}, i.e. E_g. The EQE gain of Cell C and Cell D in the long-wavelength might be attributed to the presence of high C_{Ge} (> 16.0%) regions in the light-absorbing layer as well as the strenghtened internal field beneficially to hole collection.

In Fig. 4(b), the EQE curve of Cell D with the nonlinear normal C_{Ge}-profile is compared to the cells with different types of nonlinear profilings. In the case of the cell with reverse profiling (Cell E), which has the same average C_{Ge} as the Cell D, the EQE value was considerably smaller than Cell D in the wavelength region longer than 500 nm. It is thought to be owing to the internal field enhanced in the opposite direction to hole collection for the Cell E. The EQE value of the cell with U-shape profiling (Cell F) was also samller than that of Cell D in the wavelength region (500 - 730 nm). But, in the wavelength longer than 730 nm, the light-absorption of Cell F (average C_{Ge} = 22.0%) was larger than that of Cell D due to its much larger C_{Ge}.

The results shown in Fig. 4 and Table 1, clearly demonstrate that the normal profiling is the most advantageous for improving cell performance owing to the E_g-grading in the way beneficial to hole collection as well as the advantage to utilize a wide solar spectrum although the cell performance obtained using the single-chamber PECVD in this work was relatively low compared to reported performances of nip-type a-Si:H or a-SiGe:H thin film solar cells fabricated with multi-chamber systems (Cho et al., 2011; Li et al., 2006).

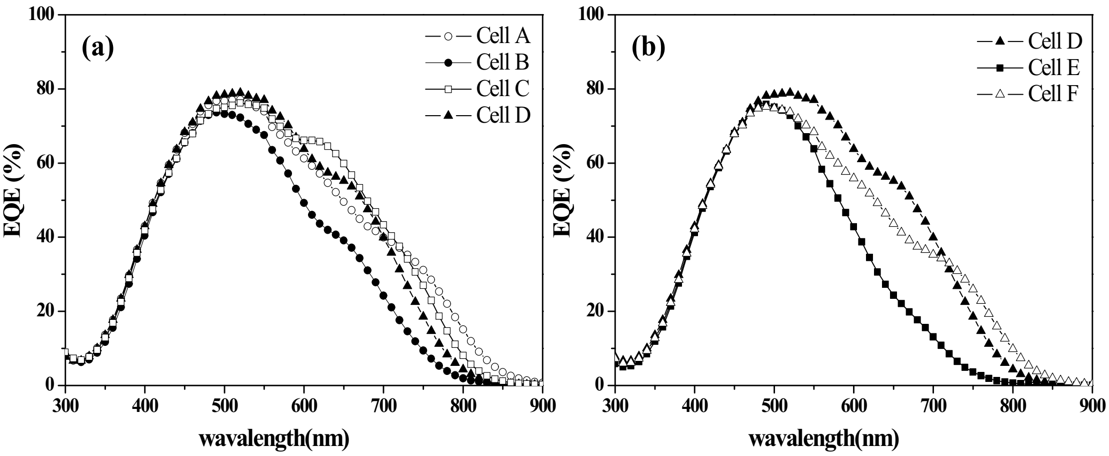

Fig. 4: EQE data of a-SiGe:H thin film solar cells listed in Table 1.

In order to consider the influence of C_{Ge}-grading on LID, the cells with C_{Ge}-constant (33.0%) (Cell A), linear normal profiling (Cell C), nonlinear normal profiling (Cell D), and nonlinear reverse profiling (Cell E) were light-soaked under 1sun at 25°C for 140 h. Fig. 5 shows the normalized FF and η as a function of light-soaking time. While there were not big differences between the cells in the V_{OC} and J_{SC} degradation behavior, the FF of Cell A was significantly decreased compared to the cells with C_{Ge}-graded profiling (Cell C, Cell D, and Cell E). Then, the η decrease of Cell A was approximately 40% while the η decrease of Cell C, Cell D, and

Cell E was approximately 25% by 140 h light-soaking. Especially, Cell C shows mostly the same LID behavior as Cell D and Cell E although the average C_{Ge} (16.5%) was considerably higher than the average C_{Ge} (11.0%) of Cell D and Cell E. The results obtained in this LID experiment clearly show that the C_{Ge}-grading in the light-absorbing layer of a-SiGe:H thin film solar cells is also advantageous for reducing LID, which has been considered to be a drawback of adding Ge in the light-absorbing layer.

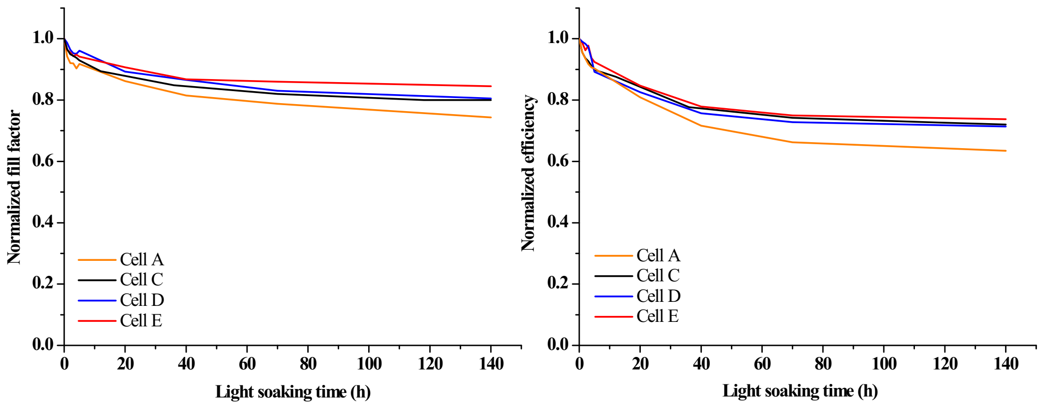

Fig. 5: Normalized FF and η of nip-type a-SiGe:H solar cells having graded C_{Ge}-profiles or constant C_{Ge} (33.0%) as a function of light-soaking time.

4. Conclusion

The influence of C_{Ge}-profiles on cell performance and LID was investigated for substrate-type a-SiGe:H thin film solar cells fabricated on opaque substrates. In this work, the cells with different C_{Ge}-profiles, such as linear normal, nonlinear normal, nonlinear reverse, and nonlinear U-shape profilings, were evaluated in comparison to that of constant C_{Ge}. The efficiency of cell with linear normal grading (average C_{Ge} = 16.5%) was 6.31% while the cells with constant C_{Ge} (16.0 and 33.0%) showed the efficiency of 4.89 and 5.24%, respectively. Among the C_{Ge}-profiles, normal profiling was found to be advantageous for enhancing light-absorption in the middle wavelength region because the E_g-grading was beneficial to hole collection. The LID experiment showed that the C_{Ge}-grading in the light-absorbing layer of a-SiGe:H thin film solar cells ~~is~~ was also advantageous for reducing LID. The use of C_{Ge}-profiling clearly shows that for nip-type a-SiGe:H solar cells, a light-absorbing layer with linear normal C_{Ge}-profiling is the most useful for obtaining high efficiency and long-term stability. The present work could suggest very useful C_{Ge}-profiling method for improving the performance of the a-SiGe:H single junction or a-Si:H/a-SiGe:H multi-junction solar cells.

5. Acknowledgement

This work was supported by the New and Renewable Energy of the Korea Institute of Energy Technology Evaluation and Planning (KETEP) grant funded by the Trade, Industry and Energy Ministry of Korea (Contract No: 20123010010150). One of the authors, S. J. Yun, was partially supported by the ETRI project (Account No: 15ZE1140).

6. References

Kondo, M., Matsuda, A., 2001. Low temperature growth of microcrystalline silicon and its application to solar cells, Thin Solid Films 383, 1-6

Xu, J., Miyazaki, S., Hirose, M., 1996. High-quality hydrogenated amorphous silicon-germanium alloys for narrow bandgap thin film solar cells, Journal of Non-Crystalline Solids 208, 277-281.

Vetterl, O., Finger, F., Carius, R., Hapke, P., Houben, L., Kluth, O., Lambertz, A., MuK ck, A., Rech, B., Wagner, H., 2000. Intrinsic microcrystalline silicon: A new material for photovoltaics, Solar Energy Materials & Solar Cells 62, 97-108.

Guo, L., Kondo, M., Fukawa, M., Saitoh, K., Matsuda, A., 1998. High Rate Deposition of microcrystalline silicon using conventional plasma-enhanced chemical vapor deposition, Japanese Journal of Applied Physics 37, 1116–1118.

Stutzmann, M., Street, R. A., Tsai, C.C., Boyce, J.B., Ready, R.E., 1989. Structural, optical, and spin properties of hydrogenated amorphous silicon-germanium alloys , Journal of applied physics 66(2), 569-592.

Beyer, W., 2010. Amorphous silicon-germanium and silicon-carbon alloys, in: Shah, A. (Eds.), Thin-film silicon solar cells. EPFL Press, pp. 76-87.

Lundszien, D., Finger, F., Wagner, H., 2002. A-Si:H buffer in a-SiGe:H solar cells, Solar Energy Materials & Solar Cells 74, 365–372.

Zimmer, J., Stiebig, H., Wagner, H., 1998. a- SiGe:H based solar cells with graded absorption layer, Journal of Applied Physics 84, 611-617.

Arya, R.R., Bennett, M.S., Rajan, K., Catalano, A., 1989. Role of interfaces on the performance and stability of amorphous silicon-germanium alloy p-i-n solar cells, Applied Physics Letters 55, 1894-1896.

Yun, S. J., Kim, J. K., Lim, J. W., 2012. Amorphous SiGe:H thin film solar cells woth light absorbing layers of graded bandgap profile, Electrochemical and Solid-State Letters 15(2), 9-12.

Shima, M., Isomura, M., Wakisaka, K., Murata, K., Tanaka, M., 2005. The influence of operation temperature on the output properties of amorphous silicon-related solar cells, Solar Energy Materials & Solar Cells 85, 167–175.

Jones, S. J., Chen, Y., Williamson, D. L., Zedlitz, R., Bauer, G., 1993. Microstructural transition and degraded opto-electronic properties in amorphous SiGe:H alloys, Applied Physics Letters 62, 3267-3269.

Zambrano, R.J., Rubinelli, F.A., Rath, J. K., Schropp, R.E.I., 2004. Computer-aided band gap engineering and experimental verification of amorphous silicon–germanium solar cells, Solar Energy Materials & Solar Cells 81, 73-86.

Agarwal, P., Povolny, H., Han, S., Deng, X., 2002. Study of a-SiGe:H films and n–i–p devices used in high efficiency triple junction solar cells, Journal of Non-Crystalline Solids 299–302, 1213–1218.

Cho, J. S., Baek, S., Lee, J. C., 2011. Surface texturing of sputtered ZnO:Al/Ag back reflectors for flexible silicon thin-film solar cells, Solar Energy Materials & Solar Cells 95, 1852-1858.

Li, H., Stolk, R. L., van der Werf, C. H. M., Franken, R. H., Rath, J. K., Schropp, R. E. I., 2006. Optimization of n–i–p protocrystalline SiGe:H thin film solar cells for application in thin film multijunction solar cells, Journal of Non-Crystalline Solids 352, 1941-1944.